

# The correlation between Physicochemical and nonlinear optical studies of tin-doped zinc oxide thin films deposited by spray pyrolysis

Amal Rherari<sup>1\*</sup>, Rahma Adhiri<sup>2</sup>, Touria Lachhab<sup>2</sup>, Mohammed Addou<sup>1,3</sup>,  
Zouhair Sofiani<sup>4</sup>, Assia Bougrine<sup>1</sup> and Kartik Kannan<sup>5</sup>

1. *Laboratory of Optoelectronic and Physical Chemistry of Materials, Ibn Tofail University, Kenitra 14000, Morocco*
2. *Laboratory of Engineering and Materials (LIMAT), Faculty of Sciences Ben M'Sik, Hassan II University of Casablanca, Morocco*
3. *Laboratory of Materials and Valorization of Natural Resources, Abdelmalek Essaadi University, FST, Tanger, Morocco*
4. *Laboratory of Thin films Materials and Photovoltaic Conversion, University Hassan II of Casablanca, FST Mohammedia, Morocco*
5. *Centre for Advanced Materials, Qatar University, P.O Box 2713, Doha, Qatar.*

(\*) E-mail: [amalrherari@gmail.com](mailto:amalrherari@gmail.com)

Received: 30/09/2021

Accepted: 02/02/2022

DOI: 10.7149/OPA.55.2.51069

## ABSTRACT:

Transparent conductive thin films based on Tin (Sn) doped zinc oxide (TZO) were prepared using the chemical spray pyrolysis technique. The crystalline structure, strain, stress, roughness characteristics, electrical and nonlinear optical susceptibility of TZO were studied. The films have been investigated using x-ray diffraction, atomic force microscopy (AFM), electrical resistivity, and third harmonic generation (THG) techniques. The greatest value of the susceptibility  $\chi^{(3)}$  was about  $10.91 \times 10^{-12}$  (esu) obtained from the 2% doped films, which have less roughness and the low electrical resistivity of  $5 \times 10^{-2} \Omega \text{ cm}$ . Moreover, third order non-linear optical susceptibilities were of the order of  $10^{-12}$  (esu), higher than that of the undoped ZnO.

**Key words:** ZnO films, Tin doping, Spray pyrolysis, roughness, THG.

## REFERENCES AND LINKS

- [1] J. Heber, "Nobel Prize 2014: Akasaki, Amano & Nakamura." *Nature Physics* 10.11 (2014): 791-791.
- [2] Y.Caglar, S. Ilican, M.Caglar, F. Yakuphanoglu, *spetctrochimica Acta Part A* 67 (2007) 1113-1119.
- [3] S. S. Shinde, A.P. Korade, C.H. Bhosade, K.Y. Rajpure, *Journal of Alloys and Compounds* 551 (2013) 688-693.
- [4] J.B. Yoo, A.L. Fahrenbruch, R.H. Bube, *J. Appl. Phys.* 68 (1990) 4694.
- [5] J.B. Baxter, E.S. Aydil, *Sol. Energ. Mat. Sol. C.* 90 (2006) 607.
- [6] D. Kim, T. Shimomura, S. Wakaiki, T. Terashita, M. Nakayama, *Phys. B* 376-377 (2006) 741.
- [7] C.Y. Liu, B.P. Zhang, N.T. Binh, K. Wakatsuki, Y. Segawa, *J. Cryst. Growth* 381 (2006) 20.
- [8] M. Mikami, T. Sato, J. Wang, Y. Masa, M. Isshiki, *J. Cryst. Growth* 286 (2006) 213.



- [9] Z. Sofiani, B. Sahraoui, M. Addou, R. Adhiri, M. Alaoui Lamrani, L. Dghoughi, N.Fellahi, B. Derkowska, W. Bala, *J. Appl. Phys.* 101 (2007) 063104.
- [10] S. Brehme, F. Fenske, W. Fuhs, E. Nebauer, M. Poschenrieder, B. Sells, L. Sieber, *Thin Solid Films* 342 (1996) 666–671. *Superlattice Microstruct.* 52 (2012) 594–604.
- [11] J.L. Van Heerden, R. Swanepoel, *Thin Solid Films* 299 (1997) 72–77.
- [12] M. Purica, E. Budianu, E. Rusu, M. Danila, R. Gavrilă, *Thin Solid Films* 403–404 (2002) 485–488.
- [13] S. Abed, M.S. Aida, K. Bouchouit, A. Arbaoui, K. Iliopoulos, B. Sahraoui *Optical Materials* 33 (2011) 968–972.
- [14] V. Kumari, V. Kumar, B.P. Malik, R.M. Mehra, D. Mohan, *Optics Communications* 285 (2012) 2182–2188.
- [15] A. Bougrine, M. Addou, A. Kachouane, J.C. Bérnède, M. Morsli, *Mater. Chem. Phys.* 91 (2005) 247–252.
- [16] J. Zou, S. Zhou, C. Xia, X. Zhang, F. Su, G. Peng, X. Li, J. Xu, *Thin Solid Films*, Volume 496, Issue 2, 21 February 2006, Pages 205–207.
- [17] K. Bahedi, M. Addou, M. El Jouad, Z. Sofiani, H. EL Oauzzani, B. Sahraoui, *Applied Surface Science* 257 (2011) 8003–8005.
- [18] M. Alaoui Lamrani, M. Addou, Z. Sofiani, B. Sahraoui, J. Ebothe', A. El Hichou, N. Fellahi, J.C. Bernede, R. Douni, *Optics Communications* 277 (2007) 196–201.
- [19] M. El Jouad, M. Alaoui Lamrani, Z. Sofiani, M. Addou, T. El Habbani, N. Fellahi, K. Bahedi, L. Dghoughi, A. Monteil, B. Sahraoui, S. Dabos, N. Gaumer, *Optical Materials* 31 (2009) 1357–136.
- [20] F.D. Paraguay, J. Morales, W. L. Estrada, E. Andrade, M. Miki-Yoshiba, *Thin Solid Films* 366 (2000) 16–27.
- [21] P. Scherrer, *Goettinger Nachr* 2 (1918) 98.
- [22] M. Sathiya, K. Ramesha, G. Rousse, S. S. Shinde, A. P. Korade, C. H. Bhosale, and K.Y. Rajpure, *J. Alloys Compd.* 551, (2013), pp. 688–693.
- [23] W. Water, S.-Y. Chu, *Materials Letters* 55 (2002) pp. 67–72
- [24] *Handbook of Chemistry and Physics*, 67th ed., CNRS, Paris, (1986–1987), p. 171.
- [25] M. Krunk, E. Mllikov, *Thin Solid Films* 270 (1995) 33.
- [26] K. Bahedi, M. Addou, M. El Jouad, Z. Sofiani, M. Alaoui Lamrani, T. El Habbani, N. Fellahi, S. Bayoud, L. Dghoughi, B. Sahraoui, Z. Essaidi, *Applied Surface Science* Volume 255, Issue 8, 1 February 2009, pp. 4693–4695.
- [27] F. Kajzar, J. Messier, C. Rosilio, *J. Appl. Phys.* 60 (1986) 3040.
- [28] M. Addou, M. El Jouad, A.M. Lamrani, Z. Sofian, B. Sahraoui, A. Monteil, N. Gaumer, S. Dabos, T. El Habbani, N. Fellahi, K. Bahedi, L. Dghoughi, 2007 ICTON Mediterranean Winter Conference, 6-8 Dec. 2007, Sousse, Tunisia (2007) DOI: 10.1109/ICTONMW.2007.4446957
- [29] R. Ghosh, D. Basak, S. Fujihara, *Journal of Applied Physics* 96, 5 (2004) pp. 2689–2692.
- [30] N. Fellahi, M. Addou, A. Kachouane, M. El Jouad and Z. Sofiani, *Eur. Phys. J. Appl. Phys.* 74 (2016) 24611.

---

## 1. Introduction

In recent years, transparent conducting oxides (TCOs) interested researchers due to their exceptional physical properties and their wide variety of applications in commercial devices, especially in data storage applications. Moreover, physics Nobel laureates succeeded in generating blue emission to fabricate the new light [1]. Among TCOs, zinc oxide is one of the most promising materials for the next generation of optoelectronic manufacturing devices [2]. Indeed, due to their wide band-gap energy, low resistivity and high transparency in the visible wavelength range, these semiconductors own high light trapping characteristics, which ensure efficient ultraviolet (UV) emission [3]. They are used as gas detectors, surface acoustic devices, transparent electrodes and solar cells [4-7]. Recently, the second and third order non-linear optical properties have been studied while the structural characteristics, electrical and optical properties of ZnO films have been widely investigated [8–12]. The possibility to get a nonlinear optical response in thin films makes them especially attractive since they can easily be used for integrated nonlinear optical devices such as optoelectronic components, optical switching, sensor protection, and optical data storage [13]. More particularly, ZnO films have strong nonlinearities with third-order susceptibility  $\chi^{(3)}$  [14], that are well suited for all these nonlinear optical applications. Furthermore, third



harmonic generation (THG) is responsible of new frequency generation starting from  $\omega$  and frequencies  $3\omega$ , via the third-order susceptibility  $\chi^{(3)}(-3\omega, \omega, \omega, \omega)$  which is symmetry-allowed in all materials [13].

Effects of doping on the several properties of tin doped zinc oxide (TZO) were reported in literature [2,15]. However, there aren't many reports on study of nonlinear optical (NLO) properties of these films. (TZO) thin films can be prepared by various deposition techniques, such as sputtering, metal-organic chemical vapor deposition (MOCVD), vapor transport, pulsed laser deposition and spray pyrolysis [2,6,7,13,15-16]. The spray pyrolysis technique has many advantages such as its simplicity, safety, and it can be adapted easily for the production of large surface films. Hence, this study investigates the correlation between crystalline structure, strain-stress relationship, surface roughness, electrical and NLO properties of THG of TZO thin films deposited on glass substrate using the chemical spray pyrolysis. This work is a continuation of previous ones on NLO properties in ZnO nanostructures [11, 17-19].

## 2. Experimental

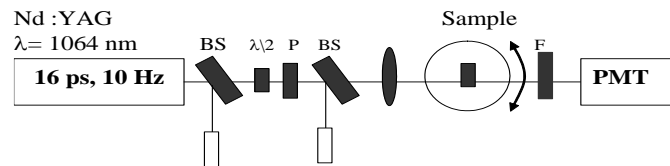


**Fig.1.** THG experimental setup: Phs: synchronization photodiode; Phc: control photodiode; k/2: half wave plate; BS: beam splitter; P: polarizer; F: transmitting filter for 355 nm; PMT: photomultiplier tube.

The spray pyrolysis set up used to obtain tin-doped zinc oxide thin films has been previously described, as well as the optimum conditions of samples preparation [15]. Original solution (0.05M) was prepared by dissolving zinc chloride ( $ZnCl_2$ ) in deionized water and tin chloride ( $SnCl_2 \cdot 2H_2O$ ) was used as the dopant compound source. The X-ray diffraction (XRD) profiles were recorded using Cu ( $K\alpha$ ) radiation in the range of  $20^\circ$ - $60^\circ$ . Morphology and roughness of the deposited films were examined by scanning electron microscope (SEM) and atomic force microscope (AFM) respectively. The latter was carried out using a Nanosurf Flex FM digital instruments operated in tapping mode. The electrical resistivity was measured at room temperature by the Van Der Paw method. The experimental setup for (THG) is presented in figure 1. It is a Q-switched mode-locked Nd:YAG laser (Model: Quantum elite) which works as the pump beam ( $\lambda = 1064$  nm) and that offers 1.62 mJ per pulse at 10 Hz; each pulse lasts 16 ps. The fundamental beam energy was controlled with a polarizer and a half wave plate focalized it on the sample through lens with focal of 25 cm. The beam diameter and the applied power density were 0.65 mm and  $2$  GW/cm<sup>2</sup> respectively. A selective filter (at 355 nm) was used to absorb the pump beam letting only the generated one being collected in a tube photomultiplier (PMT, Model: Hamamatsu). Moreover, the used density filter also reduces the generated intensity by the nonlinear sample. The third harmonic signal was detected by (PMT) which was integrated with a box-car and processed by a computer. A portion of the input beam was picked off and measured by fast photo-diode to monitor the input energy. Finally The so-called Maker-fringes were generated by rotating the sample through the range from  $\pm 40^\circ$  to the normal, giving then the values of third-order susceptibility  $\chi^{(3)}$ . Figure 2 shows Maker Fringes of silica taken as a reference material to calibrate the experimental set-up; a value of  $\chi^{(3)} = 2.62 \times 10^{-14}$  esu was used [19].

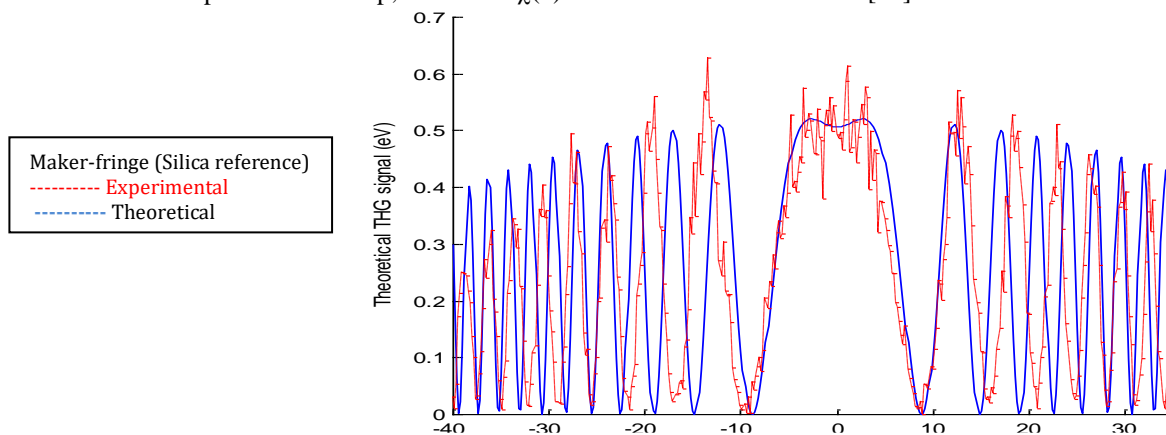


**Fig.2.** Experimental and theoretical Maker fringes of silica [19].

### 3. Results and discussion

Figure 3 shows the effects of dopant tin atoms on ZnO films. First, all diffraction peaks can be well indexed to the hexagonal phase following the same preferential direction (002) as for undoped ZnO, on the other hand, we can note that only the peaks related to the ZnO structure are present and no peak indicating the formation of tin oxide SnO<sub>2</sub> is observed. Then, we can point out that for all doping concentrations, the location of the measured diffraction peaks does not change. Nevertheless, peak intensities are more intense and sharper specially at doping ratio of 2%.

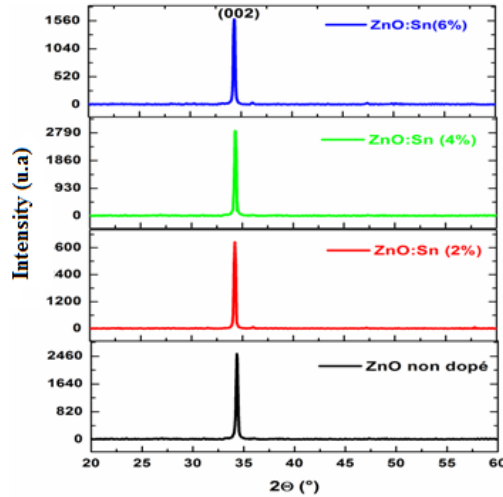


Fig.3. X-ray spectra of undoped and doped ZnO thin films for different concentrations of tin.

These results which are in good agreement with those noted by Paraguay et al [20] indicate the good crystallinity of doped films. The grain sizes  $D$  (diameters) of deposited films were estimated in the direction (002) (table 1) using Sherrer's formula [21]:

$$D = (0.9\lambda) / (\beta \cos\theta) \quad (1)$$

Where 0.9 is the shape factor,  $\lambda$  is the wavelength of incident radiation ( $\lambda = 1.542\text{\AA}$ ),  $\theta$  is the Bragg diffraction angle and  $\beta$  is the FWHM of the hkl diffraction peak measured at half of its maximum intensity (in radians).

Table 1: Lattice parameters, grain size, strain and stress of Sn-doped ZnO thin films.

Simple	Lattice constant (C-axis) (Å)	Grain size (nm)	Compression strain (%)	Elastic Constant $C_{33}^{film}$	Stress (GPa)
Pure ZnO	5.2168	31	-0.207	206.28	0.91
2% Sn-ZnO	5.2029	46	0.059	208.49	-0.26
4% Sn-ZnO	5.2244	35	-0.353	205.08	1.55
6% Sn-ZnO	5.2200	30	-0.268	205.77	1.18

Peak intensities as well as grain size are represented as a function of tin doping concentration (figure 4); it shows that the doped films at a ratio of 2% have the strongest peak and the greatest grain size. A similar effect has been reported in the work of M. Sathiya et al. [22] on tin-doped ZnO deposited by the same technique.

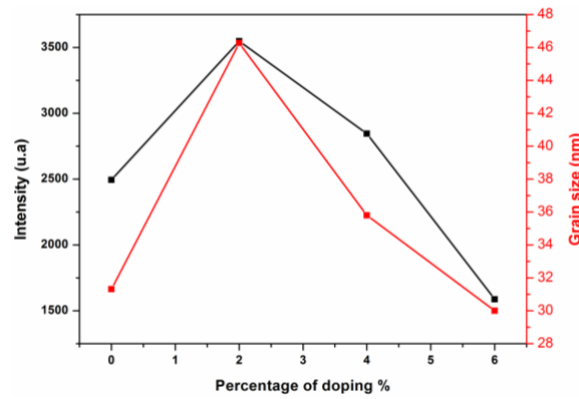


Fig.4.The variation of grain size and XRD intensity as a function of Tin doping concentration.

The two main properties extracted from peak width analysis are crystallite size and lattice strain. The biaxial strain model [23] was used to calculate the stress of the films. The strain  $e_{zz}$  along the c axis, i.e. perpendicular to the substrate surface, was obtained using equation 2:

$$e_{zz} = \frac{c_0 - c}{c_0} \quad (2)$$

Where  $c_0 = 5.206$  is the corresponding parameter taken from the ASTM sheets.

The layer stress  $\sigma$  parallel to the film surface in hexagonal lattice was derived from the relationship 3:

$$\sigma = \left[ 2C_{13} - \frac{(C_{11} + C_{12})C_{33}^{layer}}{C_{13}} \right] e_{zz} \quad (3)$$

Equation 4 was applied to obtain the elastic constant  $C_{33}^{layer}$ :

$$C_{33}^{layer} = \frac{0.99C_{33}^{crystal}}{(1 - e_{zz})^4} \quad (4)$$

The elastic stiffness constants of ZnO bulk, which have been used, are:

$C_{11} = 211.7$ ;  $C_{12} = 121.1$ ;  $C_{13} = 105.1$  and  $C_{33}^{crystal} = 201$ .

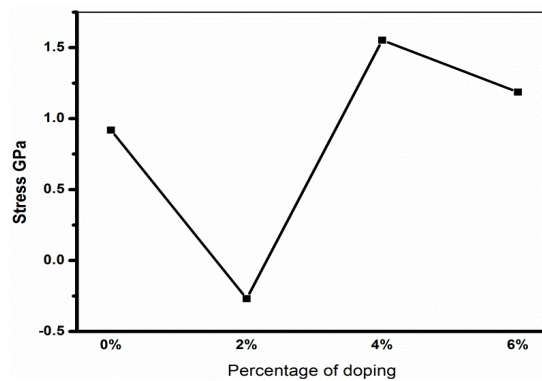


Fig.5.Evolution of the stress as a function of tin concentration.

The sources of stress in the samples are the structural defects and doping concentration. The effect of tin doping on the stress of the films is shown in Figure 5. Kumari et al [14] also observed and reported this effect. The calculated stress parallel to the films is negative only at 2% indicating that the planar stress is in compression condition at this concentration. Indeed, Figure 6 illustrates the widening of the peak (002) which shows a displacement towards the large angles for the doped layer at 2% of tin. This shift is the consequence of compression of the lattice. The calculation of the parameters  $c$ , the grain size, strain, stress and elastic constants for different concentrations of tin, are grouped together in table 1. The formula used

for the determination of the stress, is given above in the relationship (3), considering the intrinsic stress due to the structure and the density and neglecting the thermal and vibrational stresses.

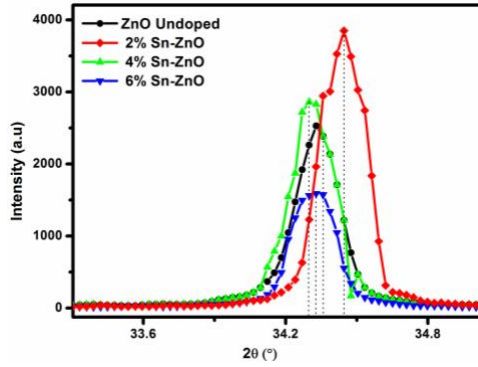


Fig.6. Peaks shift (002) with tin concentration.

Figure 7 displays the optical transmission spectra of the undoped ZnO and that of the 2% Sn samples. The transmission occurs in the visible range and is about 85% with well-contrasted interference fringes for ZnO doped Sn while it is 76% for the undoped film. This high transmission is attributed to the improvement of crystallinity [24-25].

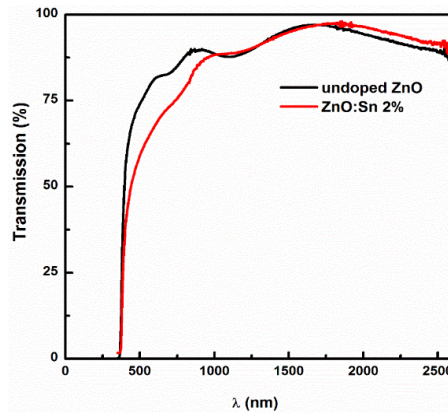


Fig.7. Transmission spectra of undoped ZnO and Sn-doped thin films.

Regarding nonlinear optical properties, the nonlinear response of TZO is more important than that of ZnO layers elaborated by other techniques [19], so it makes it the best candidate for nonlinear optical applications. The third susceptibility  $\chi^{(3)}$  has been investigated using THG technique in earlier work [26], and the harmonic signal generated in a very thin film does not exhibit losses, and dispersion. The intensity of THG is expressed through the following formula [27]:

$$I_{3\omega} = \frac{576\pi^6}{n_{3\omega}n_{\omega}^3\lambda_{\omega}^2c^2} |\chi^{(3)}|^2 I_{\omega}^3 L^2 \frac{\sin^2(\Delta kL/2)}{(\Delta kL/2)^2} \quad (5)$$

Where:  $n_{\omega}$  and  $n_{3\omega}$  are the refractive indices of the film at the fundamental frequency and the frequency of the third harmonic (TH) respectively,  $\lambda_{\omega}$  is the wavelength of the fundamental radiation,  $c$  is the speed of light in vacuum,  $L$  is the film thickness,  $\chi^{(3)}$  is the third order nonlinear optical susceptibility of the film,  $I_{\omega}$  is the power of the incident radiation and  $\Delta k$  is the wave-vector mismatch between the fundamental and TH waves in a film, given by equation 6:

$$\Delta k = \frac{6\pi}{\lambda_{\omega}} (n_{3\omega} - n_{\omega}) \quad (6)$$

It should be noted, due to the high frequencies involved, that the THG can probe purely coherent electronic nonlinearity. Figure 8 shows maker fringes for undoped ZnO (a) and 2 % Sn-doped ZnO thin



layers (b). From the THG intensities and using equation 5, nonlinear susceptibilities values are calculated then given in table 2. The third susceptibility value of Tin-doped ZnO at 2 % is two orders of magnitude higher than the reference material and matches well with those already reported for doped ZnO films [6, 7, 18]. This increase of  $\chi^{(3)}$  is attributed to the redistribution of the electronic charge density, which induce a substantial polarization. Thus, the substitution of  $Zn^{2+}$  ions by the  $Sn^{4+}$  ions (2 %) introduces an additional difference, leading to an additional polarization that allows the improvement of the nonlinear response.

**Table 2:** The Values of Third Order Non-Linear Susceptibilities for undoped and Sn-doped thin films.

Tin concentration (%)	$\chi^{(3)} \times 10^{-12}$ (esu)
0	0.93
2	10.916

Figure 9 illustrates the morphology of undoped and 2% tin-doped ZnO thin films. For the doped samples, the AFM micrograph (figure 9b) reveals a smooth surface, which confirms the good crystallized layer indicated also from the XRD results given in previous work [15]. Bahedi et al [17] have concluded previously that the surface roughness is one of the most effects acting on the nonlinear properties. Indeed, rough surfaces scatter more light from the fundamental beam thereby generating low nonlinear optical response. Moreover, the surface roughness is also associated with the optical transmission as it has already been reported [15]. Finally, the 2% ZnO: Sn appears to be the most transparent sample, exceeding 80% in the visible region. Its smoothness can anticipate less scattering light, which corresponds to good transparency and thereafter contributes to a higher nonlinear optical response [28].

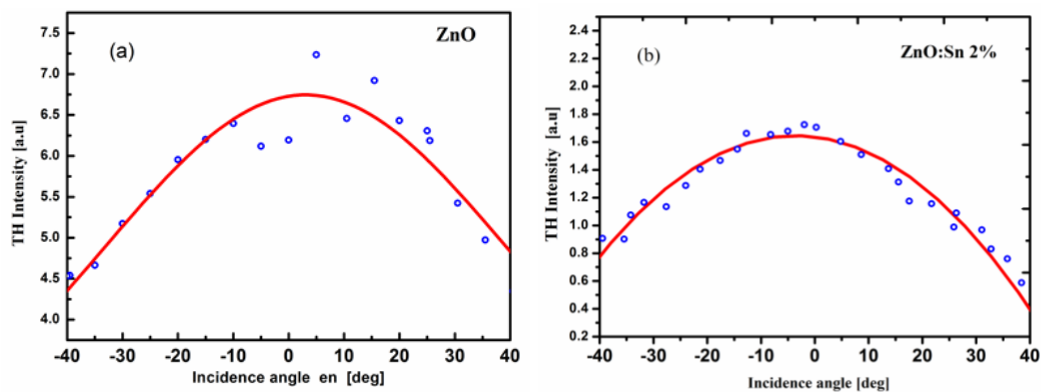


**Fig.8.** Third harmonic response for undoped ZnO (a) and 2% Sn-doped ZnO thin layers (b) deposited at 450 °C (-Fit, ... Experimental).

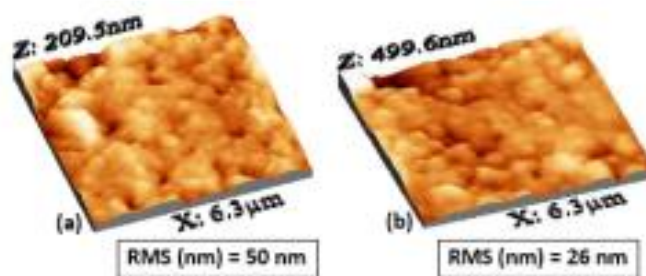


**Fig.9.** AFM images of (a) undoped and (b) 2% Sn-doped ZnO thin films.

On the other hand, according to the work of Ghorsh et al [29], the electrical properties of the transparent conductive oxides depend on their microstructure. Hence, the study of the influence of doping concentration on the resistivity of tin ZnO doped films seems of significant interest. Figure 10 shows the results of such a study at room temperature. It is obvious that tin concentration is one of the most important parameters to affect the electrical properties of these films. Initially, the resistivity decreases with doping concentration up to 2% reaching a minimum value of  $5 \times 10^{-2} \Omega \text{ cm}$ , then it increases as it has already reported in previous work [15].

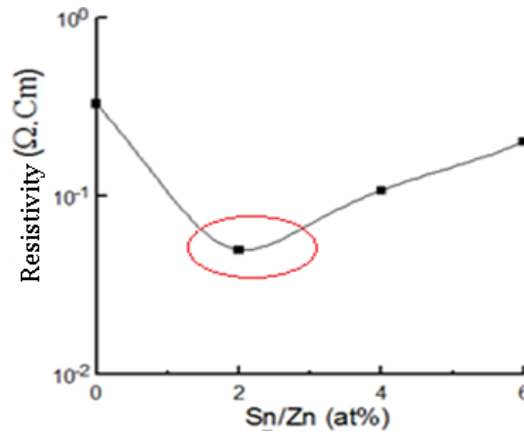


**Fig.10** Evolution of the resistivity of a ZnO layer as a function of the doping level with tin.

The high free carrier concentration in Sn doped ZnO films with a ratio of 2% is responsible of the observed low resistivity which generates a high value of the third susceptibility, confirmed by the results presented in table 2. Fellahi et al [30] has argued that the electrical resistivity is one of the most effects acting on the nonlinear properties. Indeed, when the resistivity decreases, the values of nonlinear optical properties increase. Thus, all these results allow us to conclude qualitatively that a smooth and homogenous surface combined with good crystallinity is necessary to get high third harmonic conversion efficiency, which confirms the optical transmission results already quoted in previous reports [6, 15, 17]. Moreover, when the electric conductivity increases, the value of nonlinear optical properties increases. This behavior has been confirmed already in other studies [9].

### 3. Conclusion

Highly transparent and conductive Sn-doped ZnO thin films have been obtained by the simple chemical spray pyrolysis technique and their crystalline structure, strain-stress relationship, roughness characteristics, electrical and nonlinear optical susceptibility were studied. TZO layers with resistivity as low as  $5 \times 10^{-2} \Omega \cdot \text{cm}$  were obtained for the low doping ones. The results show a strong dependence of the third order non-linear susceptibility on the surface roughness but also on the sample crystallinity and resistivity. The THG response has been measured for all studied samples and the highest value has been found for the films with a ratio of 2% in tin concentration.

**ACKNOWLEDGEMENT** :This work is supported by IsDB fellowship and PPR2015/9Morocco.